RJC

RASĀYAN ***J. Chem.***
Vol. 18 | No. 1 |275-284| January - March | 2025
ISSN: 0974-1496 | e-ISSN: 0976-0083 | CODEN: RJCABP
http://www.rasayanjournal.com
http://www.rasayanjournal.co.in

GREEN SYNTHESIS OF COPPER NANOPARTICLES FROM MANILA TAMARIND SHELL: CHARACTERIZATION, ANTIMICROBIAL STUDIES, AND PHOTOCATALYTIC DEGRADATION

Dasari Kiran Kumar✉ and Pulipati King
Department of Chemical Engineering, Andhra University College of Engineering (A), Andhra University, Visakhapatnam-530003, Andhra Pradesh, India.
✉Corresponding author: dasarikirankumar018@gmail.com

ABSTRACT

There are numerous possible uses for green nanoparticle synthesis in the biological and environmental sciences. Green synthesis strives to reduce the use of harmful chemicals in particular. For example, using organic resources like plants is usually safe. Studied the basic principles of green chemistry, the synthesis of nanoparticles mediated by plants, and their recent applications. Plants additionally consist of decreasing and capping agents. Nanoparticles include copper, palladium, platinum, zinc, gold, silver, etc. Fourier transform infrared spectroscopy (FTIR), scanning electron microscopy (SEM), ultraviolet-visible spectroscopy, and X-ray diffraction (XRD) were utilized to examine the green-produced Manila Tamarind Shell Copper nanoparticles (MTS-Cu NPs). With FTIR, the existence of several functional groups was identified. The size range, according to SEM analysis, is 88–152 nm. UV visible spectroscopy was used to find out the absorbance of 0.4942 and the maximum wavelength is 308 nm. This study showed that green MTS Copper Nanoparticles could be applied in the future to remove colors from contaminated water in addition to serving as an antioxidant and antibacterial agent. Gram-negative bacteria were shown to have a higher maximal ZOI than gram-positive bacteria. This efficiency was significantly higher than that of typical antibiotics such as Oxacillin (20 mm vs. 25 mm) for Staphylococcus aureus, Ampicillin (18 mm vs. 22 mm) for Escherichia coli, and Ciprofloxacin (16 mm vs. 20 mm) for Pseudomonas aeruginosa. The plant known as "Manila Tamarind" can be inexpensively and efficiently used to produce Cu NPs for a variety of purposes. The synthesized Cu NPs exploited as photocatalysts exhibited excellent degradation efficiency on organic dyes Methylene Blue and Malachite Green under sunlight. The calculated degradation efficiencies for Methylene Blue and Malachite Green were 90% and 85%, respectively. The rate constants for the Methylene Blue and Malachite Green dyes were found to be 0.0215 min^{-1} and 0.0153 min^{-1}respectively.

Key Words: MTS, Green Synthesis, Kinetic Studies, Antimicrobial Studies, Cu NPs

RASĀYAN *J. Chem.*, Vol. 18, No. 1, 2025

INTRODUCTION

Nanoparticles, with their interesting properties emerging from their small size (1-100 nanometers), have reformed different fields including gadgets, medication, ecological remediation, and energy creation. Nonetheless, conventional combination techniques frequently depend on brutal synthetics and energy-concentrated processes, raising worries about natural poisonousness, asset consumption, well-being dangers, and cost adequacy. Moreover, these strategies frequently need command oversize and morphology, restricting their expected applications.[1,2] Green blend offers an additional supportable and harmless to the ecosystem elective. This approach uses the force of normal living beings like plants, microorganisms, and organisms, which go about as both decreasing and covering specialists, to integrate nanoparticles without unforgiving synthetic compounds.[3,4,5] Their powerful cancer-prevention agent properties offer possible applications in safeguarding against oxidative pressure and related sicknesses. Moreover, their synergist capacities hold a guarantee for speeding up compound responses and improving modern cycles, prompting expanded productivity and decreased energy utilization.[6] Manila Tamarind Shell (MTS), a promptly accessible side-effect with inborn decreasing and covering properties, is a promising contender for green blends, especially for copper nanoparticles (Cu NPs). Cu NPs have a few groundbreaking properties, including strong antimicrobial movement against a scope of microbes and parasites, making them important in battling anti-microbial safe microorganisms and creating novel

http://doi.org/10.31788/RJC.2025.1819057

antimicrobial specialists.[7,8,9,10] This examination expects to open the capability of MTS in green Cu NP amalgamation and investigate their different applications. The primary goal includes fostering an enhanced green combination convention for proficient and reproducible Cu NP creation utilizing MTS extricate. Portraying these CuNPs utilizing progressed strategies like Ultraviolet-Visible Spectroscopy, X-ray diffraction (XRD), Fourier Transform Infrared Spectroscopy (FTIR), and Scanning Electrode Microscope (SEM) will uncover their size, morphology, crystallinity, and practical gatherings. Thinking about the antimicrobial movement in contrast to different microorganisms and growths will survey their true capacity to fight irresistible sicknesses. Moreover, investigating their cancer prevention agent movement will open entryways for their utilization in medical services and different fields.[11,12,13,14] At long last, researching their likely application in water sanitization holds a guarantee for tending to clean water shortage and guaranteeing maintainable water assets. In general, this exploration tries to lay out MTS as a significant asset for green nanotechnology and open the maximum capacity of Cu NPs for a better and cleaner future.[15,16,17] Zinc oxide nanoparticles effectively removed alizarin red S from hydrous solutions, with the highest adsorption capacity of 123.3 mg/g, despite not being entirely successful.[18] The study used Cu/ZnO NPs as an adsorbent to remove Congo red, resulting in a maximum CR adsorption of 94.14% and desirability of 0. 976.[19] Using XRD, SEM, and FTIR testing, the study creates Allium sativum skin/zinc oxide nanoparticles as an adsorbent to remove Congo red, a hazardous azo dye.[20] The study created A. cepa-ZnO NPs, a green zinc oxide nanoparticle synthesis that effectively destroys toxic colors and has antibacterial capabilities, highlighting its potential for environmental remediation.[21] The study successfully eliminated nitrate from aqueous solutions using an iron plate electrode and electrocoagulation, attaining the greatest efficiency under certain pH, time, and temperature conditions.[22] The article describes an electrocoagulation process for treating phosphate-contaminated water utilizing iron and aluminium plates, with the iron plate electrode achieving the maximum removal efficacy of 93.94%. [23]

EXPERIMENTAL

Materials and Methods

After purchasing Copper Sulphate Pentahydrate ($CuSO_4.5H_2O$) from Sigma Aldrich, it was utilized without any additional purification. Shells from Manila Tamarinds were gathered in the Narsapur forest in Medak District. The copper sulfate solution and plant extract were made with double-distilled water. The workspace and all of the tools utilized, including the UV spectrophotometer, beakers, Eppendorf tubes, funnels, and falcon tubes, were sterile.

General Procedure

Preparation of *Manila Tamarind Shell* Extract

Samples of Manila Tamarind Shells are shown in Fig.-1. Samples of Manila Tamarind Shells were subjected to washing with distilled water and grinding to fine pieces and 20g of MTS powder was dropped into 100ml. double distilled water, mix well and heat for 45 minutes. in a hot water bath. The extract was then filtered using whatmanNo.41 filter paper to obtain Manila Tamarind shell aqueous extract and for future usage, the filtrate was refrigerated.

Synthesis of Cu-NPs

For four hours at room temperature (27^{o}C), 4 g of copper sulfate pentahydrate and 100 cc of Manila Tamarind shell aqueous extract were combined with magnetic stirring. Within ten minutes, the blue hue of copper sulfate pentahydrate turned brown, signifying the creation of Cu NPs as a result of the reduction of copper ions from Cu (II) ions to Cu metal. The samples were then centrifuged for 10 minutes at 3000 rpm to get a clear, room-temperature supernatant. For FTIR, SEM, and XRD examination, in an oven, the copper nanoparticles were dried. for four hours at 80 to 90 degrees Celsius. Figure-2 displays the comprehensive synthesis and characterization flow sheet.

Detection Method

Characterization

To completely comprehend the green-integrated Cu NPs utilizing MTS extricate, different procedures were utilized. UV-noticeable spectroscopy affirmed their development with a top at 308 nm, demonstrative of

their size and dissemination. XRD uncovered their translucent construction with sharp pinnacles relating to a face-focused cubic gem grid. FTIR distinguished utilitarian gatherings on their surface, proposing MTS's job in covering and adjusting. At long last, SEM pictures showed their circular shape with a typical size of 20-30 nm, affirming size consistency and interaction control. Joining these investigations gave a thorough comprehension of the MTS-Cu NPs' properties, pivotal for the enhancement, fitting, and opening of their expected applications.

Fig.-1: Manila Tamarind Shell

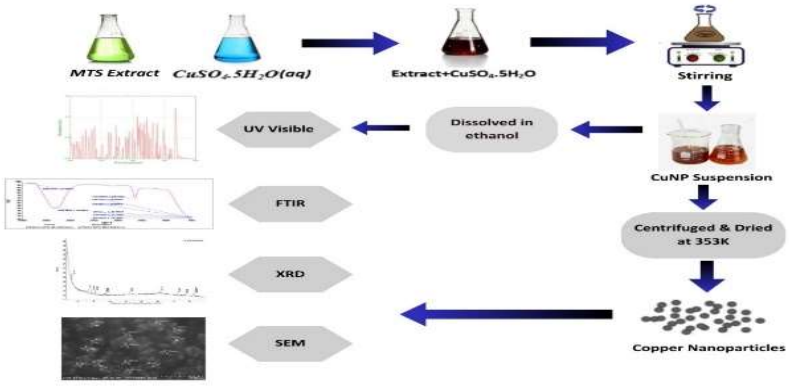

Fig.-2: Schematic Diagram of Synthesis and Analysis of MTS-Cu Nanoparticles

RESULTS AND DISCUSSION

Ultraviolet-Visible Spectroscopy

UV–Vis or UV/Vis stands for Ultraviolet-Visible Spectroscopy or Ultraviolet-Visible Spectrophotometer. Absorption spectroscopy or reflectance spectroscopy in portions of the ultraviolet and the entire, neighboring visible spectrum ranges is discussed in Fig.-3, 4, and 5. It is concerned with the investigation of matter's interaction with light. The foundation of spectroscopy is the measurement of an atom or molecular sample's spectrum, which is a graph showing the strength of radiation emitted or absorbed by the sample as a function of frequency or wavelength. It employs light in the visible and neighboring ranges, according to this. The apparent hue of the compounds involved is directly influenced by their absorption or reflectance in the visible spectrum.[14,15] The domain of visible radiation spans from 10 nm to 400 nm, and the region of UV radiation is from 400nm to 800nm.

Fluorescence spectroscopy and absorption spectroscopy are complementary in that fluorescence deals with transitions from the excited state to the ground state, whereas absorption measures transition from the ground state to the excited state. The UV-visible absorbance Spectrum recorded for MTS-Cu NPs exhibited λ_{max} of 308 as shown in (Fig.-5). This absorption band is mostly caused by MTS-Cu NPs' surface plasmon resonance. A similar result was obtained after examining generated Cu NPs with Ocimum sanctum leaf extract. Because surface plasmon absorbance varies with NP size, each study reports a different max value for NPs manufactured using different plant extracts.

Scanning Electron Microscope (SEM)

In a scanning electron microscope (SEM), a concentrated electron beam is used to scan the surface of a sample, generating pictures of the material. The sample atoms and electrons interact to produce a variety of signals that reveal details about the sample's composition and surface topography.

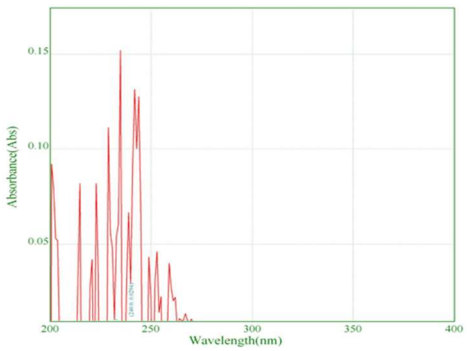

Fig.-3: Wavelength $CuS0_4.5H_2O$

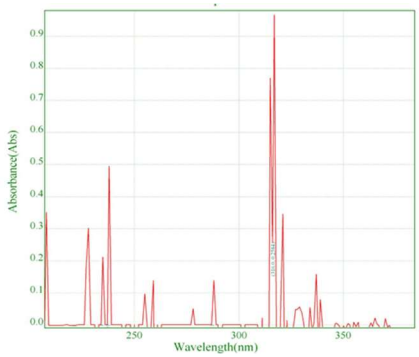

Fig.-4: Wavelength MTS

Maximum Wavelength(nm): 240 Absorbance (Abs): 0.2584

Maximum Wavelength(nm): 316 Absorbance (Abs): 0.0294

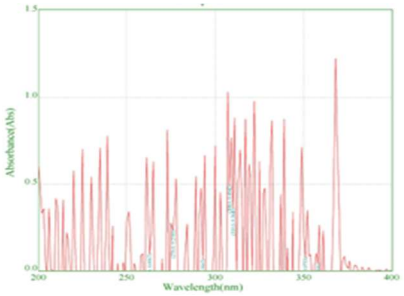

Fig.-5: Wavelength *MTSCu-NPs*

Maximum Wavelength(nm): 308, Absorbance (Abs): 0.4942

The strength of the detected signal is combined with the position of the electron beam as it scans in a raster scan pattern to produce an image. Using a secondary electron detector (Everhart-Thornley detector), secondary electrons released by atoms stimulated by the electron beam are found in the most popular SEM mode. Specimen topography affects the quantity of detectable secondary electrons and, thus, the signal strength. The SEM (Scanning Electron Microscope) image displayed in Fig.-6 illustrates the various sizes and tiny structures of MTS-Cu NPs. For the best imaging, it offers steady probe currents and great resolution. The SEM results of the MTS-Cu NPs Scanning Electron Microscope (SEM) show the particle size in the range of 88.7 nm to 152 nm.[24]

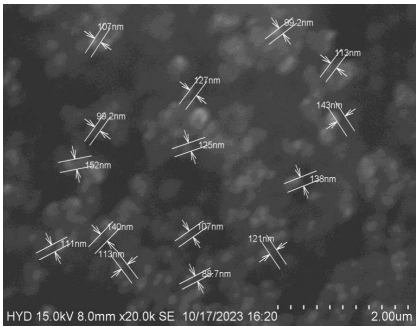

Fig.-6: SEM Analysis of MTS-Cu NPs

Fourier Transform Infra-Red Spectroscopy (FTIR)

A method for obtaining an infrared spectrum of a solid, liquid, or gas's absorption or emission is called Fourier transform infrared spectroscopy, or FTIR. High-spectral-resolution data throughout a broad spectral range is concurrently collected by an FTIR spectrometer. Compared to a dispersive spectrometer, which measures intensity over a limited range of wavelengths at a time, this offers a substantial benefit. In order to be analyzed using a Fourier transform infrared spectrometer equipped with a SHIMADZU IR Prestige - 21 Intron magnifying equipment using the transmittance mode works with a resolution of 4 cm^{-1}, a sample

of dried Cu nanoparticles is combined with KBr. The FTIR Spectra obtained (Fig.-7) for the Manila Tamarind Shell extract and MTS extract capped Cu nanoparticles reveal that: The peak at 3338.18 cm $^{-1}$ a strong broad peak is assigned to -OH stretching vibrations of alcohol Compounds in the extract. The sharp peak at 1632.90 cm^{-1} clearly indicates the C=C stretching's.[13] Hence from the IR spectra, it is evident that MTS-Cu are capped with organic molecules present in the extract.

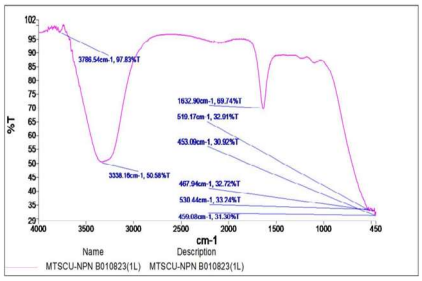

Fig.-7: FTIR Analysis of MTS-Cu NPs

X-Ray Diffraction

The crystallinity and composition of the produced MTS-Cu NPs were revealed by the X-ray diffraction (XRD) pattern. The X-ray diffraction (XRD) composition and crystallinity image are shown in Fig.-8. The pattern exhibits sharp peaks at 2 theta values of 42.28° and 76.89°, This can be related to copper nanoparticles' (Cu NPs') face-centered cubic (fcc) structural structure.[7,25] This indicates the successful formation of crystalline Cu NPs in the sample. Additionally, a peak observed at a 2-theta value of 61.17° suggests the presence of copper oxide (CuO) alongside the Cu NPs.[25,26] This finding indicates that the green synthesis process using Manila Tamarind Shell extract might have partially oxidized some of the Cu NPs, resulting in the formation of CuO. The presence of both Cu NPs and CuO within the MTS-Cu NPs signifies their potential for applications requiring a mixture of these two materials. Further analysis and optimization of the synthesis process could be conducted to tailor the relative proportions of Cu NPs and CuO for specific applications.

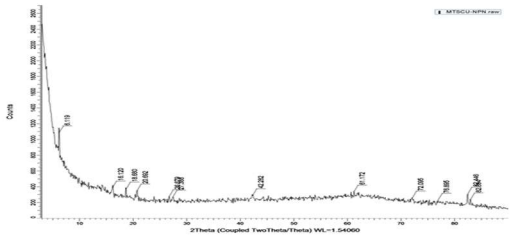

Fig.-8: X-Ray Diffraction Graph of MTS-Cu NPs

Antimicrobial Studies

This study investigated the antimicrobial activity of Manila tamarind shell (MTS) capped copper nanoparticles (Cu NPs) against various pathogenic bacteria (Table-1). Figure-9 depicts a comparison image of the fluctuation of the zone of inhibitions at different bacterial pathogens. The zone of inhibition assay revealed that MTS-Cu NPs exhibited potent antibacterial activity at a concentration of 40 mg/ml. When compared to common antibiotics, such as Oxacillin (20 mm vs. 25 mm) for Staphylococcus aureus, Ampicillin (18 mm vs. 22 mm) for Escherichia coli, and Ciprofloxacin (16 mm vs. 20 mm) for Pseudomonas aeruginosa, this effectiveness was much greater (Fig.-10).

Table-1: Zone of Inhibition (mm)

Microorganism	MTS CuNPs (mm)	Standard Antibiotic (mm)
Staphylococcus	20	25
E. coli	18	22
Pseudomonas aeruginosa	16	20

These findings unequivocally show that MTS-Cu NPs have the potential to be a viable substitute for traditional antibiotics, providing a long-term and efficient means of treating infectious infections brought on by these bacterial strains. The release of copper ions (Cu^{+2}) can interact via electrostatic attraction with

the bacterial cell wall, which explains the enhanced antibacterial activity of MTS-Cu NPs. These Cu^{+2} ions also have the ability to pass through bacterial membranes and interfere with vital cellular functions, which in turn causes bacterial death. This study offers strong proof of the exceptional antibacterial agent.

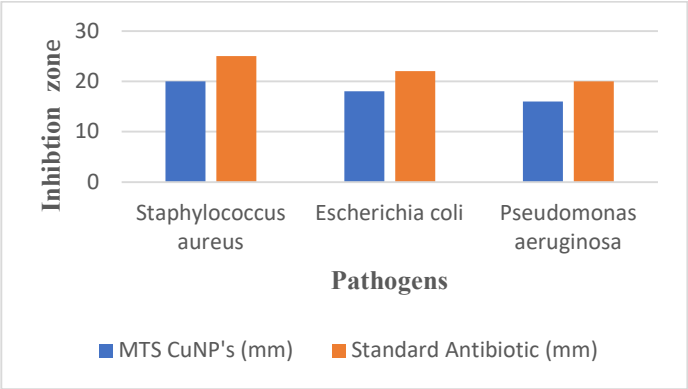

Fig.-9: Antibacterial Activity: The Variety of Inhibitory Zones for Various Bacterial Pathogens

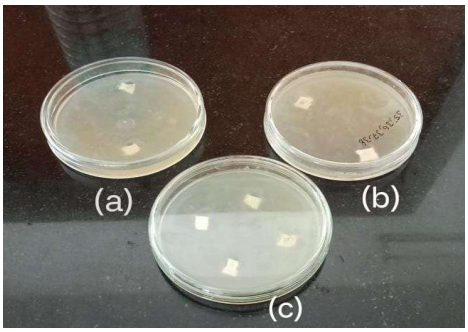

Fig.-10: Cu NPs' Antimicrobial Activity Against E. coli (a), Pseudomonas Aeruginosa (b), and Staphylococcus Aureus (c)

Photocatalytic Degradation of Methyl Blue and Malachite Green using MTS-Cu NPs

The photocatalytic degradation efficiency of MTS-Cu NPs for both methyl blue (MB) and malachite green (MG) was evaluated under direct sunlight irradiation. The characteristic absorption peak intensity of each dye decreased over time in the presence of MTS-Cu NPs, indicating their degradation. The photocatalytic activity was quantified using a spectrophotometer at the maximum absorbance wavelengths of Methylene Blue at 664 nm and Malachite Green at 618 nm. The experiment employed an initial dye concentration of 10 mg/L and a MTS-Cu NPs dosage of 10 mg. This efficient degradation highlights the potential of MTS-Cu NPs for wastewater treatment applications.[27,28] The photodegradation process was significantly enhanced at a basic pH (pH = 7) for both dyes. This can be attributed to the influence of pH on the surface charge properties of the MTS-Cu NPs and the dye molecules. At basic pH, the negatively charged dye molecules are more prone to adsorption onto the positively charged photocatalyst surface, facilitating degradation. The calculated degradation efficiencies for Methylene Blue and Malachite Green were 90% and 85%, respectively, as shown in Fig.-11 and 12. Control experiments were conducted to eliminate the possibility of self-degradation, adsorption alone, or MTS-Cu NP activity in the dark. Negligible degradation was observed in the absence of light or catalyst, confirming that a photocatalytic process was responsible. This process can be summarized as follows:

$$Cu + h\upsilon \rightarrow Cu\,(e^{-}h^{+}) \quad \text{(i)}$$
$$Cu + h\upsilon \rightarrow Cu\,(e^{+}) + Cu(h^{+}) \quad \text{(ii)}$$
$$Cu(e^{-}) + O_2 \rightarrow O_2^{-} \quad \text{(iii)}$$
$$Cu(h^{+}) + H_2O \rightarrow OH^{-} \quad \text{(iv)}$$
$$O_2^{-} \text{ or } OH^{-} + \text{Dye} \rightarrow \text{degraded product} \quad \text{(v)}$$

Steps in the Photocatalytic Degradation

Light Absorption

MTS-Cu NPs absorb solar radiation due to the surface plasmon resonance (SPR) effect, leading to the excitation of electrons (Eq.-i).

Charge Carrier Generation

The excited electrons and holes can participate in redox reactions (Eq.-ii and iii).

Radical Formation

The electrons react with oxygen (O_2) to generate superoxide radicals (O_2^-) (Eq. (iii)), while holes react with water (H_2O) to produce hydroxyl radicals ($OH^{\cdot}$) (Eq.-iv).

Degradation

These highly reactive radicals ($O2^-$ and $OH^{\cdot}$) interact with the dye molecules (Methylene Blue (MB) or Malachite Green (MG)), causing their breakdown into smaller molecules (Eq.-v).

The literature supports the dominance of hydroxyl radicals in dye degradation using nanoparticles.[29] This aligns with the observed photocatalytic activity of MTSCu NPs.The pseudo-first-order kinetic model was applied to describe the photocatalytic decolorization process. The linear relationship between ln(Ct/C₀) and irradiation time (t) in Fig.-13 and 14 confirm this model's validity.[29]

$$ln\ C_t/C_0 = -\ kt$$

Where, C_0 is the initial concentration of dye, C_t is the concentration at the irradiation time (t) and k is the rate constant ($min.^{-1}$).

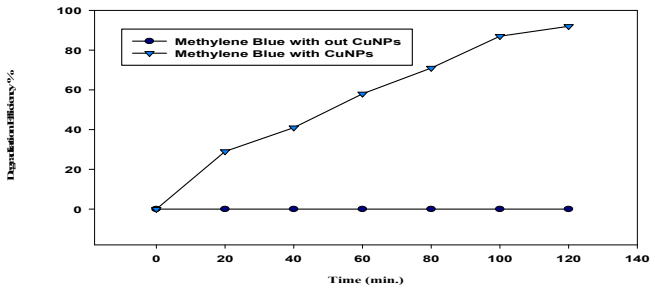

Fig.-11: Photocatalytic Degradation Efficiency of Methylene Blue Under Sunlight Irradiation

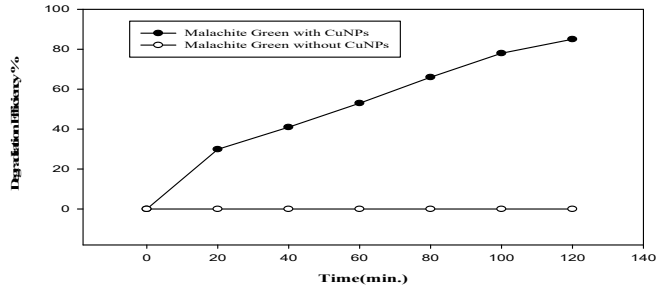

Fig.-12: Photocatalytic Degradation Efficiency of Malachite Green under Sunlight Irradiation

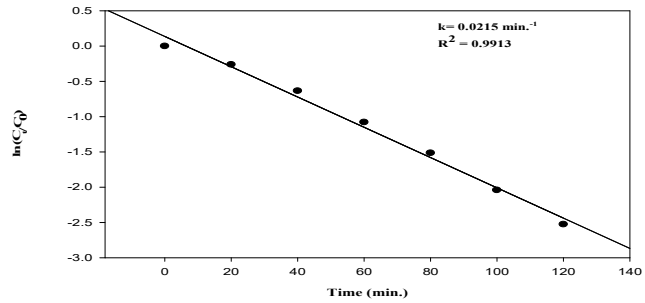

Fig.-13: Kinetic Data for the Degradation of Aqueous Methylene Blue under Sunlight Irradiation

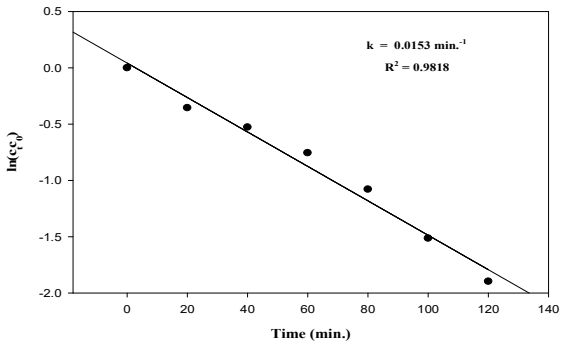

Fig.-14: Kinetic Data for the Degradation of Aqueous Malachite Green under Sunlight Irradiation

The rate constants (k) were calculated to be 0.0215 min^{-1} for Methylene Blue and 0.0153 min^{-1} for Malachite Green, indicating efficient degradation by MTS-Cu NPs. These values are comparable to those reported for other photocatalysts, as shown in Table-2.

Table-2: Comparison of Photocatalysts for Dye Degradation

S. No.	Photocatalyst	Degradation Time (min)	Reference
1	AuNPs	8	27
2	AgNPs	45	11
3	SnO_2 NPs	70	30
4	$rGO/TiO_2/CO_3O_4$ NPs	120	31
5	Sb-ZnO NPs	210	32
6	CuNPs	120	This work

MTS-Cu NPs demonstrate promising photocatalytic activity for degrading Methylene Blue and Malachite Green under sunlight irradiation. The efficient degradation, influence of pH, and confirmation of the photocatalytic mechanism suggest their potential for wastewater treatment applications. Further studies could optimize the reaction conditions and explore the reusability of MTS-Cu NPs for practical applications.

CONCLUSION

For the first time, copper nanoparticles were successfully produced utilizing a unique *Manila Tamarind shell (MTS)* for the anti-bacterial investigation, which provides a cost-effective, simple, and efficient method for the production of Cu NPs. FTIR analysis indicated the presence of a functional group in the leaf extract. These functional groups were primarily responsible for the reduction of copper metal ions into Cu NPs. The produced copper nanoparticles were examined with an XRD, FITR, SEM, and UV spectrophotometer. The X-ray diffraction (XRD) pattern exhibits sharp peaks at 2 theta values of 42.28° and 76.89°, this is because copper nanoparticles (CuNPs) have a crystal structure of face-centered cubic (fcc). The FTIR Spectra obtained for the Manila Tamarind Shell extract and MTS extract capped Cu nanoparticles reveal that: The peak at 3338.18 cm^{-1} a strong broad peak was assigned to -OH stretching vibrations of alcohol compounds in the extract. The sharp peak at 1632.90 cm^{-1} clearly indicates the C=C stretching's. The SEM results of MTS-Cu NPs Scanning Electron Microscope (SEM) show the particle size in range of 88.7 nm to 152 nm. Copper nanoparticles were successfully used in the antibacterial activity investigation. Gram-negative bacteria were shown to have a higher maximal ZOI than gram-positive bacteria. This efficiency was significantly higher than that of typical antibiotics as Oxacillin (20 mm vs. 25 mm) for Staphylococcus aureus, Ampicillin (18 mm vs. 22 mm) for Escherichia coli, and Ciprofloxacin (16 mm vs. 20 mm) for Pseudomonas aeruginosa. The plant known as "Manila Tamarind" can be inexpensively and efficiently used to produce Cu NPs for a variety of purposes. The synthesized Cu NPs exploited as photocatalyst exhibited excellent degradation efficiency on organic dye Methylene Blue and Malachite Green under sunlight. The calculated degradation efficiencies for Methylene Blue and Malachite Greenwere 90% and 85%, respectively. The rate constants for the Methylene Blue and Malachite Green dyes were found to be 0.0215 min^{-1} and 0.0153 min^{-1}respectively. The dye adsorption results were compared with previously reported literature. The overall study revealed that Cu NPs successfully

synthesized by green route and used as photocatalyst and antibacterial agents. The plant known as "Manila Tamarind" can be inexpensively and efficiently used to produce Cu NPs for a variety of purposes.

ACKNOWLEDGEMENTS

I express my sincere gratitude to B.V. Raju institute of technology for providing access to their well-equipped laboratory facilities, enabling the successful execution of experiments crucial to this research paper.

CONFLICT OF INTERESTS

There is no conflict of interest, according to the authors.

AUTHOR CONTRIBUTIONS

All the authors contributed significantly to this manuscript, participated in reviewing/editing and approved the final draft for publication. The research profile of the authors can be verified from their ORCID ids, given below:

Dasari Kiran Kumar https://orcid.org/0000-0002-8719-7613
Pulipati King https://orcid.org/0000-0001-8210-3019

REFERENCES

1. F. A. M. Alahdal, M. T. A. Qashqoosh, Y. K. Manea, R. K. A. Mohammed, and S. Naqvi, *Sustainable Materials Technologies*, **35,** e00540(2023), https://doi.org/10.1016/j.susmat.2022.e00540
2. Z. Alhalili, *Arabian journal Chemistry,* **15(5)**, 103739(2022), https://doi.org/10.1016/j.arabjc.2022.103739
3. M. K. Ghosh, S. Sahu, I. Gupta, and T. K. Ghorai, *RSC Advance*, **10(37)**, 22027(2020), https://doi.org/10.1039/D0RA03186K
4. M. A. A. Al-Khafaji, R. A. K. Al-Refai'a, and O. M. Y. Al-Zamely,*Material Today Proceeding*, **49**, 2831(2021), https://doi.org/10.1016/j.matpr.2021.10.067
5. H. C. A. Murthy, T. Desalegn, M. Kassa, B. Abebe, and T. Assefa, *Journal of Nanomaterials*, **2020(1)**, 3924081(2020), https://doi.org/10.1155/2020/3924081
6. S. C. Mali, A. Dhaka, C. K. Githala, and R. Trivedi, *Biotechnology Reports*, **27**, e00518(2020), https://doi.org/10.1016/j.btre.2020.e00518
7 S. Amaliyah, D. P. Pangesti, M. Masruri, A. Sabarudin, and S. B. Sumitro, *Heliyon*, **6(8)**, e04636(2020), https://doi.org/10.1016/j.heliyon.2020.e04636
8. P. A. Nguyen, A.V. P. Nguyen, T.D. Bao, H.P.Phan, T.T.V Nguyen, B. A. Tran, T.L.D Huynh, T. C.Hoang, V.T Huynh and T.Nguyen., *Discover Applied Sciences*, **2**, 1795(2020), https://doi.org/10.1007/s42452-020-03539-8
9. S. Ahmed, Saifullah, M. Ahmad, B. L. Swami, and S. Ikram, *Journal Radiation. Research and Applied Sciences.*, **9(1)**, 1(2016), https://doi.org/10.1016/j.jrras.2015.06.006
10. S. Adewale Akintelu, A. Kolawole Oyebamiji, S. Charles Olugbeko, and D. Felix Latona, *Current Research in. Green and Sustainable Chemistry.*, **4**, 100176(2021, https://doi.org/10.1016/j.crgsc.2021.100176
11. C. J. De Andrade, L. Andrade, M. Mendes, and C. Nascimento, *Global Journal of Researches in Engineering C Chemical Engineering*, **17**, 27(2017),
12. R. G. Saratale, G.D Saratale, H. S. Shin, J. M. Jacob, A Pugazhendhi, M. Bhaisare, and G.K. Kumar, *Environmental Science and Pollution Research.*, **25**, 10164(2018), https://doi.org/10.1007/s11356-017-9912-6
13. H. Khoshsang, K. Abbasi, and A. Ghaffarinejad, *Inorganic Chemistry Communications*, **155**, 111083(2023), https://doi.org/10.1016/j.inoche.2023.111083
14. D. Mott, J. Galkowski, L. Wang, J. Luo, and C.-J. Zhong, *Langmuir*, **23(10)**, 5740(2007), https://doi.org/10.1021/la0635092

15. A. M. Fayaz, K. Balaji, M. Girilal, R. Yadav, P. T. Kalaichelvan, and R. Venketesan, *Nanomedicine: Nanotechnology, Biology, Medicine*, **6(1)**, 103(2010), https://doi.org/10.1016/j.nano.2009.04.006
16. N. Sreeju., A. Rufus, and D. Philip, *Journal of Molecular. Liquid.*, **221**, 1008(2016), https://doi.org/10.1016/j.molliq.2016.06.080
17. M. Marszewski, S. Cao, J. Yu, and M. Jaroniec, *Materials Horizons*, **2(3)**, 261(2015), https://doi.org/10.1039/C4MH00176A
18. B. Sowjanya, U. Sirisha, A. Suhasini Juttuka, S. Matla, P. King, and M. Vangalapati, *Material Today Proceeding*, **62**, 3968(2022), https://doi.org/10.1016/j.matpr.2022.04.576
19. B. Sowjanya, P. King, M. Vangalapati, and V. R. Myneni, *International Journal of Chemical Engineering*, **2023**, 8640288(2023), https://doi.org/10.1155/2023/8640288
20. B. Sowjanya, P. King, and M. Vangalapati, *European Chemical Bulletinl*, **2023,** 326(2023) https://doi.org/ 10.31838/ecb/2023.12.si5.039
21. S. Bandela, P. King, M. Vangalapati, and V. Myneni, *Chemical Papers*, **78,** 5209(2024), https://doi.org/10.1007/s11696-024-03459-6
22. V. Supriya, B. Sowjanya, D. Kiran Kumar, V. R. Poiba, and M. Vangalapati, *Material Today Proceeding*, (2023), https://doi.org/10.1016/j.matpr.2023.05.154
23. V. Supriya, B. Sowjanya, D. Kiran Kumar, L. Ramadevi, V. Rao Poiba, and M. Vangalapati, *European Chemical Bulletinl,* **2023**, 333(2023), https://doi.org 10.31838/ecb/2023.12.si5.040
24. Y. Abboud, T. Saffaj, A. Chagraoui, A. El Bouari, K. Brouzi, O. Tanane and B. Ihssan**e**, *Applied Nanoscience*, **4**, 571(2014), https://doi.org/10.1007/s13204-013-0233-x
25. V. Gopalakrishnan and S. Muniraj, *Material Today Proceeding*, **36**, 832(2021), https://doi.org/10.1016/j.matpr.2020.07.013
26. A. Lanje, S. Sharma, R. Pode, and R. Ningthoujam F. N. A. Sc, "Synthesis and optical characterization of copper oxide nanoparticles," *Advances in Applied. Science. Research.*, **1(2)**,36(2010).
27. B. Paul, B. Bhuyan, D. Dhar Purkayastha, M. Dey, and S. S. Dhar, *Materials Letters*, **148**, 37(2015), https://doi.org/10.1016/j.matlet.2015.02.054
28. A. Sharma and R. K. Dutta, *RSC Advance*, **5 (54)**, 43815(2015), https://doi.org/10.1039/C5RA04179A
29. R. Singh and S. Dutta, *Advanced Powder Technology*, **29(2)**, 211(2018), https://doi.org/10.1016/j.apt.2017.11.005
30. G. Elango and S. M. Roopan, *Journal of Photochemistry and Photobiology B: Biology*, **155**, 34(2016), https://doi.org/10.1016/j.jphotobiol.2015.12.010
31. R. Ranjith, V. Renganathan, S. M. Chen, N. S. Selvan, and P. S. Rajam, *Ceramics International*, **45(10)**, 12926(2019), https://doi.org/10.1016/j.ceramint.2019.03.219
32. L. Chen,I Batjikh, J. Hurh, Y. Han, Y. Huo, H. Ali, J. Feng Li, E.J. Rupa, J.Chan Ahn, R. Mathiyalagan, and D. C. Yang , *Optik*, **184,** 324(2019), https://doi.org/10.1016/j.ijleo.2019.03.051

[RJC-9057/2025]